BEAM DUMPS, ENERGY SLITS AND COLLIMATORS AT SLAC -- THEIR FINAL VERSIONS AND FIRST PERFORMANCE DATA*

D. R. Walz, L. R. Lucas, H. A. Weidner, R. J. Vetterlein, E. J. Seppi
Stanford Linear Accelerator Center, Stanford University, Stanford, California

Summary

This paper discusses the final as-built versions of high power beam dumps, slits and collimators, which are capable of absorbing 1 to 2 MW electron beams continuously. Some of the important design features are illustrated with pictures. Experimental results of testing a beam dump window and a small module prototype are added. The remote control and read-out system of variable aperture slits and collimators is emphasized and performance data are given. Then the criteria for safely achieving high beam power dissipation (heat transfer rates, nucleate and film boiling conditions, thermal stress, thermal shock and fatigue) are reviewed. Solutions to problems encountered in operating equipment in a corrosive, high radiation area where organic lubricants fail are presented. Finally, radiolysis of water and evolution of free hydrogen are dealt with. Experimental results from high power electron beams are reported. Disposal of hydrogen and radioactive gases evolving in surge tanks is discussed and solutions are proposed.

High Power Beam Dumps

A detailed description of the SLAC high power beam dumps has been published[1] and only the criteria and a summary are presented here. The water-cooled beam dumps are designed to dissipate an average power of 2.2 MW for the range of 11 to 25 GeV from an incident electron beam which may vary in diameter from 0.2 to 1.0 cm. A total of 30-radiation lengths (r.ℓ.) of material is needed to absorb and fully attenuate the beam. The beam develops its shower maximum within a vortex flow of water in the 10-r.ℓ. long front section of the dump (see schematic Fig. 1). The 20-r.ℓ. long rear section of the dump, consisting of water-cooled, chromium-plated copper plates further attenuates the electromagnetic cascade shower.

The actual beam dump prior to installation is shown in Fig. 2. The right hand side of this front view shows the water inlet manifold at the top, then the water outlet manifold, and a drainage line at the bottom. The dump vessel and external piping are fabricated from stainless steel type 316-L. This material was selected because of its superior corrosion resistance. It is a fully austenitic, low-carbon steel which is Mo-stabilized. Carbide precipitation in the multitude of welds is negligible and corrosion resistance in these highly sensitized areas is superior. Furthermore, type 316-L appears to be less susceptible than type 304 to stress corrosion cracking, the frequent swift destroyer of stainless structures. The water quality of the primary, i.e., radioactive water loop, is monitored daily. A resin ion-exchanger located in a bypass loop serves to keep the water at 1 MΩ-cm, or better. The ph is slightly acidic, about 6.2 to 6.5. Particular attention is given to chlorides in the water, since they are a major factor in initiating stress corrosion cracking in stainless steels. Concentrations of chlorides are < 1 ppm. To date, after 8 months of continuous operation, no failures have occurred. A major concern for maintenance work has been the radiation from curies of Be^7 (54 days half-life) which will be formed in the radioactive water loops under high-power operation. Measurements have indicated that essentially all the Be^7 is trapped in the ion-exchanger, thus localizing the radiation problem and making it easy to shield against.

The beam enters into the dump vessel through a 0.125 cm thick, hemispherically shaped, hard chrome-plated copper window. The window is located in the downstream end of the vacuum pipe, shown to the left in Fig. 2. Such a window was tested in the National Bureau of Standards' Linac and is described in more detail below.

The highest average power yet deposited and dissipated in the A-Beam dump was 175 kW at 16.3 GeV (on 1/21/67). The dump performed as expected. At this power level radiolysis in the water causes formation of a significant amount of free hydrogen, described in detail below.

Slits and Collimators

Several basically different types of slits and collimators are used in the SLAC beam transport system. All devices are located in the beam switchyard.

High-Power, Low-Z Slit and Collimator

A variable opening high-power collimator is used to define the spatial extent of the electron or positron beam at the beginning of the beam switchyard. It can also be used simply as an aperture stop in the transport system. The collimator is formed by placing two slits at 90°.

A high-power slit is presently used in the beam transport system supplying the research area in End Station A. The slit has a variable aperture and provides a stop for momentum transmission in the beam. (The dispersion at the slit due to the first bending magnet group is 0.15%/cm.) The slit material is basically low-Z. The reasons for selecting water and aluminum are high energy deposition rates, resulting heat fluxes, and thermal stresses (discussed in earlier publications[1,2,3]). The low-Z of these materials also helps to keep down induced radioactivity, an important factor in accessibility to slit and collimator locations.

Design Features

The high-power slit is capable of continuously absorbing up to 2.2 MW of average beam power for beam radii, $\sigma_b \geq 0.3$ cm and up to 1 MW for $\sigma_b \geq 0.1$ cm. The slit is 30-r.ℓ. (≈5 m) long, and it was assembled from modular sections for fabrication and alignment reasons. Typical modules are shown in Fig. 3. Aluminum alloy 6061-T6 was selected as the module material for its high strength, good thermal conductivity, and corrosion resistance.[4] The minimum wall thickness between the vacuum interface and the cooling water passages is 0.125 cm.

A total of 11 modules are assembled to a strongback to form a jaw, and two opposing jaws form a slit. Figure 4 shows a partially completed vertical slit. Each module floats axially with respect to the strongback on linear ballbushings; this allows for thermal expansion between strongback and power absorbing modules. The strongback is used as water inlet manifold and its temperature remains essentially constant during operation. Only the last module is rigidly connected to the strongback

* Work supported by the U.S. Atomic Energy Commission.

via the water inlet pipe, and all modules on one jaw are in series in the water loop. The beam-defining plane formed by the front face of all the modules was aligned flat to ± 0.015 cm. A double pantograph assembly (parallogram linkage) is employed to provide centerline stability. The link between two opposing pantographs is made with high-strength, low-stretch aircraft cables, Fig. 5. Spherical ball-journals connect pantograph arms and strongback. These allow differential gap opening between front and rear of the slit jaws which may be used to accommodate for angular divergence of the beam. The convolutions on the modules are the result of heat transfer requirements.[1,3] Proper assembly of two opposing jaws allows nesting of modules, i.e., no line-of-sight is possible and a slit can be used as a beam stopper.

Each slit assembly is placed in a vacuum tank and operated by means of two actuators attached to the front and back of one jaw. The tank in turn is supported by a rigid frame which can be adjusted normal to the beam direction with mechanical precision jacks. This allows positioning of the slit to ± 0.003 cm. The vacuum in the slit tank is approximately 10^{-5} torr.

Low Power, High-Z Slits and Collimators

Variable aperture, low-power, high-Z slits and collimators were designed and built to serve as back-up devices for the high-power units. Two collimators and two slits are now in use: A collimator immediately upstream of the high-power collimator, a photon beam collimator, and two slits for momentum definition in the two beams serving the major research areas. These slits are capable of continuously absorbing up to 40 kW of average power for beam radii $\sigma_b \geq 0.3$ cm and up to 20 kW for $\sigma_b \geq 0.1$ cm. They are fabricated from forged OFHC copper; the slit length is 47.5 cm. Each jaw consists of one water-cooled copper module, attached to a pantograph assembly (similar to the one described above). Aperture adjustments are possible only as parallel translations about a common centerline. Small physical size made it possible to locate both slits of a collimator in one vacuum tank.

An interesting feature is the "coil-spring" water manifold. The maximum possible aperture opening is 15 cm, i.e.,7.5 cm translation for each jaw. Physical and stroke limitations make bellows a poor choice as flexible link in the water supply and return lines. Thus the "coil-spring" water manifold was developed. Everdur piping was bent into a coil-shape and brazed to the modules. Hardness lost at the joints during brazing was restored by shot-peening. A prototype coil was cycled 10^5 times to assure that fatigue is not a limiting factor. Figure 6 shows the horizontal slit of the high-Z collimator.

Functioning of all the high-Z units has been faultless to date. The significant difference between the Z of high-power and high-Z slits as well as a large difference in physical length should make it possible to partially answer questions of the influence of these parameters on slit scattering and beam halo formation.

Remote Control and Position Read-Out

Two types of adjustments can be made on each slit: (a) Remotely controlled adjustments during beam operation, such as opening and closing of the slit aperture; (b) semi-remote and manual adjustments on maintenance days, performed in the tunnel; this covers all alignment operations and is done solely by mechanical jacks.

All remotely controlled adjustments are accomplished from the Data Assembly Building (DAB). A group of panels in the DAB houses the controls, read-outs and warning lights for the electric motor, electromagnetic clutches, shaft encoders, potentiometers and limit switches, all of which are contained in a "drive control box." This box is located in the upper tunnel housing in the vicinity of each slit, outside the very high radiation environment. The drive control box is connected to the jack-actuator at the slit via drive shafts, universal joints, and angle gear boxes.

Electromagnetic clutches allow operations in both fast and slow drive modes. The fast mode enables full-range adjustment in less than one minute and is used to get into the vicinity of the desired location. Then the slow mode is used for accurate positioning. Least count accuracy is 0.0035 cm for the collimator and 0.014 cm for the slit (based on full aperture opening). Backlash in the various drive components adds ≈0.002 cm. Hysteresis was measured to be up to 0.013 cm for high power slits and was negligible for high-Z slits. Reproducibility of aperture width and centerline of the 5 m long slit of ±0.03 cm has been achieved. Assurance concerning the actual location of each slit and its centerline is obtained in three different ways: (a) Second level optical survey is used to position each slit with respect to an external reference. Tooling balls and mirror stages, rigidly mounted to the external structure of the slit, were set during assembly and have known distances and rotations with respect to the slit centerline. Precision alignment jacks allow adjustments to 0.003 cm accuracy; (b) the two slits of the collimator (as well as the high-Z collimator) are connected to laser beam target stations. A tooling ball and mirror stage mounted externally on the laser target station defines its position with respect to the tooling balls on the slit. The laser beam and Fresnel targets allow positioning of the slit such that its centerline coincides with the electron beam centerline; (c) the electron beam can be used as a survey tool to ascertain such information as rotation of the slit about an axis normal to the beam centerline, comparison of centerline location of high-Z and high power collimators or slits. An analysis of the electron beam spectrum is also possible. In all cases, two steering magnets deflect the beam across the front face of the slit, and beam current transmission is measured as a function of magnet current. Differences of 0.005 cm can be detected Figure 7 shows a spectrum obtained with the high-Z B-Beam on 2/1/67 for a 6 GeV beam.

Window and Module Tests

Beam Dump Window

As indicated above, a full-size prototype of a beam dump window was tested in the National Bureau of Standards' Linac. Thermocouples were attached to the airside of the window. The highest beam power transmitted was 38 kW from a beam having E_o = 85 MeV, I_{peak} = 270 mA, pulse length = 5.5×10^{-6} sec, repetition rate = 300 pulses/sec. The heat transfer rate from the window to the water was approximately 1.25 kW/cm^2 in the area of beam impingement. The highest temperature recorded was ≈315°C on the air surface of the window. This thermocouple did not, however, coincide with the beam centerline and temperatures may have been as high as 350° C. The power thus dissipated by the window corresponds to approximately five times the power expected from transmitting a 10 GeV, 2.2 MW electron beam into the A-Beam dump at SLAC. The window showed no spallation effects due to thermal shock, and the hard chromium plating on the water side appeared to be undamaged.

Slit Module

A small prototype of an aluminum slit module was tested for thermal shock in the Astron accelerator at LRL in Livermore. This high intensity machine can produce bursts of very high power density over short periods of time. The highest power density was achieved by a beam of E_0 = 3.8 MeV, I_{peak} = 90 A, pulse length=0.3 μsec, rep. rate = 5 pulses/sec and beam diameter = 1 cm. This resulted in a local heat flux from the 0.125 cm thick module wall of approximately 115 Watts/cm^2. Much more spectacular than this average heat flux, however, is the rate of energy deposition during the pulse. This instantaneous heat dissipation gives rise to very steep temperature gradients in space and time, resulting in proportional thermal stress gradients. Large thermal stress gradients can cause formation of thermal shockwaves, which in turn can result in fracture and spallation of materials, regardless of how well the part is cooled. For the aforementioned run the rate of energy deposition during the pulse in the module wall was 600,000 kW/cm^3. Although very high in comparison with such values from other accelerators, this power deposition was not high enough to damage the aluminum alloy. No effect on the module wall was visually detectable after several hours of beam exposure. Thus, even for a well focused SLAC beam, no thermal shock and spallation problems are expected for slits and collimators.

Criteria for High Beam Power Dissipation

The extremely high power densities of the SLAC Linac and possible future accelerators gives rise to very high volume energy deposition rates. For example, a 20 GeV, 2.2 MW incident beam of 0.6 cm diameter deposits 198 kW/cm^3 at the shower maximum in copper. Clearly, excessive temperature rises and gradients result for any practical geometry. Experiments have shown that local heat fluxes of 2 to 3 kW/cm^2 can be safely dissipated by nucleate and film boiling into water for materials with good thermal conductivity. Selection of low-Z materials is required to make fabrication and successful operation possible. Low-Z materials will result in reasonable temperature gradients and keep thermal stresses at levels for which favorable thermal fatigue properties still exist. High strength materials with a reasonable hardness will suffer much less from the effects of cavitation erosion[1] in regions of high heat fluxes than do low strength, soft materials. Corrosion resistance of materials to be water-cooled should be high to minimize costly shutdowns. Rigid control of water purity is essential.

Friction and Wear in a High Radiation Environment

Remote control and actuation systems usually contain some rolling or sliding parts subject to friction and wear. Expected high radiation prohibits the use of organic lubricants, and inorganic, dry lubricants are often not useful either. Moreover, ionizing radiation will cause formation of a corrosive atmosphere containing nitric acid and possibly other oxidants.

Experiments were conducted at SLAC to evaluate promising material pairs. The goal was to find corrosion resistant materials which can slide and roll dry, unlubricated, at minimum clearances, without galling or seizing and which show minimum wear and are corrosion resistant. The vital part of the experimental apparatus consisted of a 1.5-inch diameter shaft rotating under 80 lbs. load in a 1.5-inch long sleeve bearing at 8 rpm. All experiments were done in air and at room temperature. Selection of material pairs was according to known friction and wear criteria. Dry friction always causes wear, but hard materials wear less than soft ones. Materials should have high moduli of elasticity, high recrystallization temperature and resistance to plastic flow in order to minimize galling and seizing. A hardness of at least Rockwell C-42 appears to be required. Furthermore, a lamellar structure as found in dry lubricants such as molybdenum and tungsten disulfides and diselenides, graphite and others is desirable. Slip between low shear strength layers causes formation of lamellar particles and hexagonal lattice structure has just this property. Attention was focused on finding and evaluating corrosion resistant, high strength materials having hexagonal lattice structure. Cobalt and titanium alloys performed remarkably well. Stainless steel 440-C hardened to Rockwell C-56 made an excellent compatible material pair with the α-titanium alloy Ti-5A1-2.5Sn. Stainless steel 440-C and Stellite No. 6 (Co-28 Cr-4W) also formed a very good material pair. Moreover, the experiments have shown that for these hexagonal materials it is not necessary to have dissimilar materials in the pair. Material pairs where both the shaft and the sleeve bearing were composed of stainless steel 440-C, Stellite No. 6 or α-titanium alloy (Ti-5A1-2.5 Sn) performed very well. A selected material pair was considered a success if it survived 10^4 cycles without seizing for clearances < 0.006 cm. Successful operations with clearances as low as 0.0018 cm were achieved. For compatible materials, the minimum clearance is determined by the size of the wear particles and equilibrium surface roughness. If a material pair is compatible, it will establish its own characteristic equilibrium surface roughness regardless of the initial surface finish of each individual material. Having thus established compatible material pairs, dry lubricants can be used to lower the coefficient of friction, depending on application. But because of the thinness of dry lubricant film they can not be relied on for successful operation; they are just an added bonus. No wear failures in the slit and collimator actuation system have occurred to date.

Radiolysis and Hydrogen Evolution

Theory: In the SLAC energy absorbers large quantities of water are used as the coolant and primary energy absorbant. Particularly in the high power beam dumps the electromagnetic cascade shower is primarily developed in water. Solid materials (copper plates) are not encountered until the resultant particles of the shower have been well attenuated. At E_0 = 20 GeV the primary electrons, upon traversing through a volume of water, gradually lose their energy as a consequence of radiation effects and collisions with atomic electrons. The most important processes are radiation, Compton scattering, pair production and ionization. For electrons with energies $E_0 > 0.5$ MeV, the linear energy transfer, short L.E.T., i.e., the amount of energy lost per unit distance travelled is $-dE/dx \approx 2$ MeV/cm. This energy is lost in discrete amounts averaging about 100 eV per event. In the region where this energy transfer occurs water molecules are excited; this region is called a spur. For this case spurs will be an average of 5000Å apart.[5] During the pulse, high concentrations of free radicals such as H and OH are thought to be formed in the spur. Some of these radicals will react with one another; others may diffuse out of the spur into the bulk water. The reactions within the spur will yield H_2, H_2O, H_2O_2 and others. The radicals diffusing into the bulk can increase in concentration to a point where they not only react with the H_2, H_2O, and H_2O_2, but also with one another to form more H_2 and H_2O_2. Since the solubility of hydrogen in water is only about 0.8×10^{-3} moles/liter, there will after a certain time be a net evolution of free hydrogen. Also, once equilibrium concentration is reached, hydrogen peroxide is expected to decompose due

to radiation and other chemical reactions and a net production of O_2 can be expected. Theoretical quantitative prediction of evolution rates is a complicated task. It is thought that at least 14 rate equations have to be solved simultaneously and many of the rate constants are not yet determined.

Experiments: Other experimenters[6] have made measurements to determine the amount of free hydrogen produced using a pulsed electron linac for pulses $\approx 7 \times 10^4$ rads and energies $E_0 \approx 15$ MeV. A constant yield of $G = 0.71$ (Molecules H_2/100 eV) was observed by Andersen and Hart. Hart predicted[7] that this yield would be constant for pulses in the range of 10^2 to 10^7 rads. Using $G(H_2) = 0.70$ results in a total rate of H_2 evolution of 1.6 liters/(MW sec) from the SLAC high-power dump. Whether or not this G-value holds at much higher energies and current densities than reported above has not been determined. However, it is thought[8] that the true value will lie within a factor of two of $G = 0.70$, which would amount to a range of 0.8 to 3.2 ℓH_2/(MWsec). Impurities contained in any real, operating water system have a marked effect on reaction rates and may influence $G(H_2)$ significantly. Experiments were performed at SLAC to measure the rate of H_2 evolution in the high-power beam dump. About 90% of the energy entering the dump is dissipated directly in the water, with the remaining approximately 10% dissipated in the copper plates and a very small part lost from the system due to radiation. The beam dump radioactive water system is a closed loop system with a surge tank, pump and heat exchanger. Hydrogen produced by radiolysis evolves in the aerated gas space on top of the surge tank and its concentration is measured in a sampling loop. H_2 evolution was evaluated for electron energies of 10.0, 12.0 and 16.3 GeV, pulses of 6×10^6 to 5.4×10^7 rads and average power into the dump ranging from 20 kW to 170 kW. The rates of H_2 evolution varied from 0.26 to 0.44 ℓ/(MW sec) with an average of 0.31 ℓ/(MW sec). The latter corresponds to $G(H_2)_{av} = 0.14$. It seems that at these high energies and power densities new, yet unknown, reactions occur which tend to favor recombination of free radicals to form H_2O rather than H_2, H_2O_2 and possibly O_2. More data will be taken in the near future to substantiate the G-value. The free hydrogen evolving in the surge tanks presents real problems. The lower explosive limit of a hydrogen-air mixture is at 4% H_2 for atmospheric conditions (STP). One can consider 2% H_2 the upper limit for safe, continuous operation. For water already saturated with H_2 it took only 10 minutes to reach the safe limit at $P_{av, H_2O} = 150$kW. A simple solution would be to dilute the gases coming off the surge tanks and vent them into the atmosphere. Unfortunately, even at low average power levels of say 50 kW the amount of radioactivity released into the atmosphere is prohibitive for any long-term operation. The SLAC Health Physics Group has measured the gases on top of the surge tank during several experiments and identified O^{15} (2 minutes) and C^{11} (20.5 minutes) as major contributing isotopes. A drying column failed to remove the O^{15}, suggesting that it is in gaseous form (O_2) rather than in the H_2O molecules of the water vapor. Chemical removal of CO and CO_2 indicated that virtually all C^{11} is in CO_2. Two possible solutions for removal of evolved hydrogen are presently being evaluated: (a) a chemical CO_2 removal-storage-venting system, and (b) a catalytic recombination system. In the first system gases coming off the surge tanks are diluted to achieve concentrations of < 2% H_2. Then CO_2, i.e., C^{11}, is removed in a resin bed. Thereafter, the gases pass through a storage area (tank) large enough to guarantee a lapse time of 12 to 15 half-life periods for O^{15} before they are finally vented into the atmosphere. The second suggested solution would consist of a fully closed system in which the gases are diluted to maintain concentrations of < 2% H_2. The gases are continuously recirculated through a catalytic bed, in which H_2 and O_2 are recombined to form water.

Acknowledgements

The authors would like to express their sincere appreciation to the members of the Mechanical Engineering and Fabrication Group for their efforts in the design and fabrication of the energy absorbers. A dept of gratitude is owed to E. L. Garwin, R. E. Taylor and J. Jurow for the many valuable suggestions during the developmental stage, to L. Cooper, J. Mitchell, W. Scott, J. Wagner and I. Zavialoff for their efforts during the design stage, and to L. Cain and J. Ryan for their work and support during fabrication.

References

1. D. R. Walz, J. Jurow, and E. L. Garwin, "Water Cooled Beam Dumps and Collimators for the Stanford Linear Accelerator," IEEE Transactions on Nuclear Science, Vol. NS-12, No. 3, June 1965. Also, SLAC-PUB-95, March 1965.
2. D. R. Walz, "Heat Transfer and Thermal Stress Analysis of Slits and Collimators," SLAC Internal Report TN-64-29 (1964).
3. L. R. Lucas and D. R. Walz, "Heat Transfer and Thermal Stresses in Tube-Forest Slits and Collimator," SLAC Internal Report TN-64-61 (1964).
4. D. R. Walz, "Corrosion in an Aluminum-Stainless Steel System," SLAC Internal Report TN-64-17 (1964).
5. A. O. Allen, "The Radiation Chemistry of Water and Aqueous Solutions," D. vanNostrand Co., Princeton (1961).
6. A. R. Anderson and E. J. Hart, J. Phys. Chem. Vol. 66, p. 70 (1962).
7. E. J. Hart, Argonne National Laboratory Report No. UAC-7229 (1963).
8. D. K. Nichols, M. T. Simnad and V. A. J. VanLint, General Atomic Division of General Dynamics, San Diego, California (private communication).

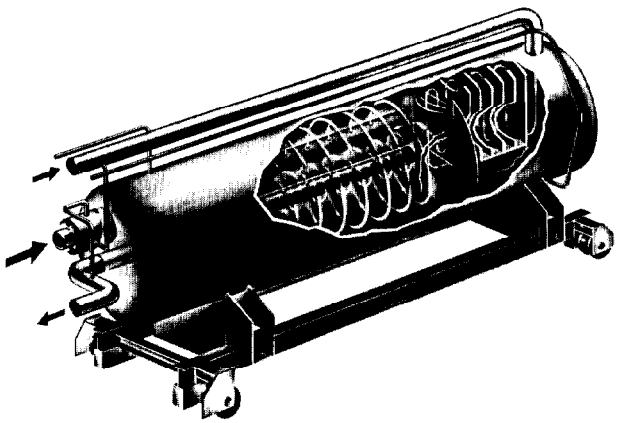

Fig. 1. Artist's Conception of 2.2 MW Beam Dump.

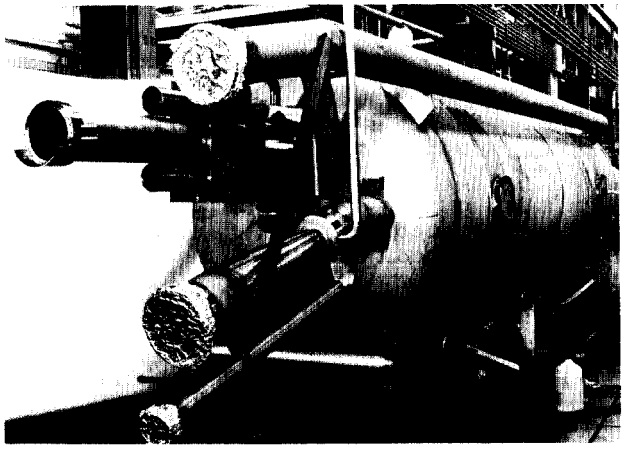

Fig. 2. Front View of Beam Dump.

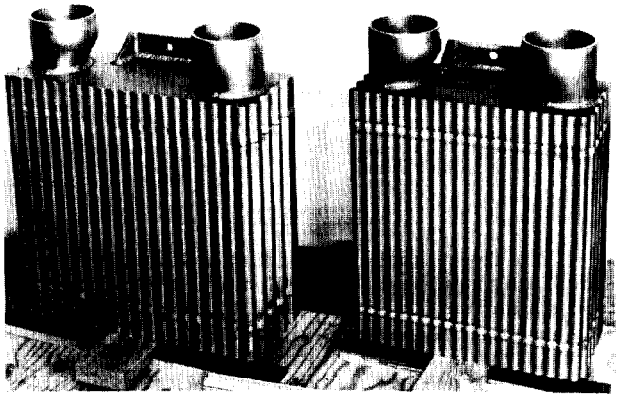

Fig. 3. Collimator Modules.

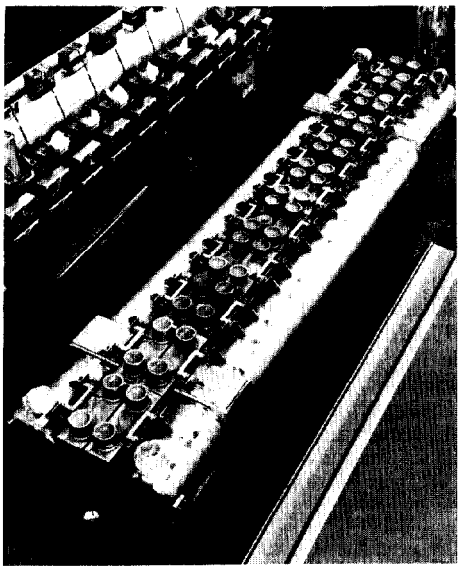

Fig. 4. Module-Strongback Assembly.

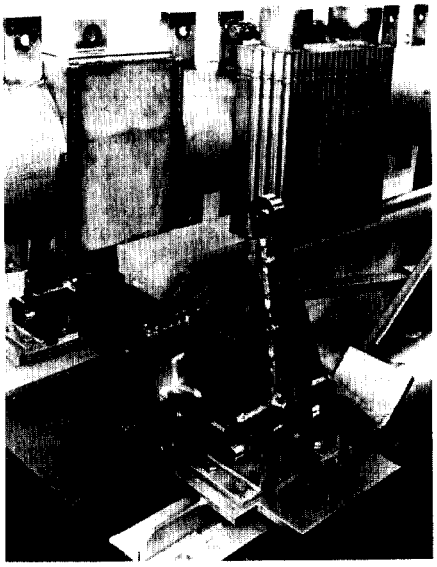

Fig. 5. Strongback-Pantograph Assembly.

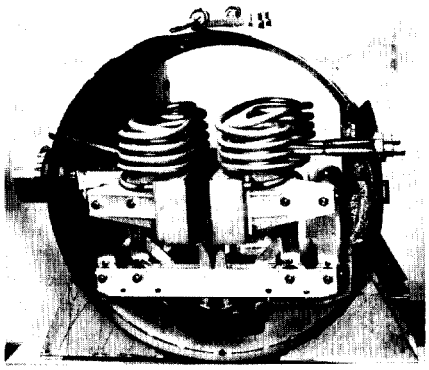

Fig. 6. High-Z Collimator (Horizontal Slit).

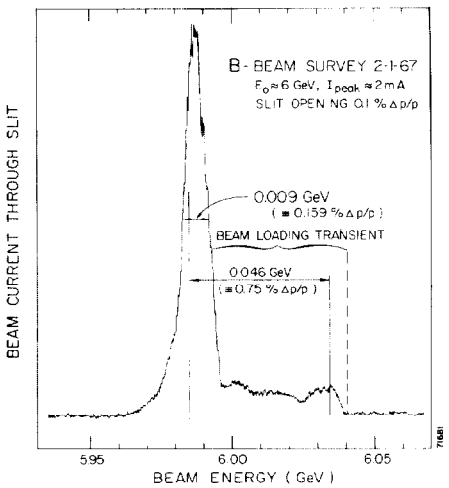

Fig. 7. Spectrum for 6 GeV Beam.